

## PHOTO-INDUCED ELECTRON TRANSFER REACTIONS

## STUDIED BY FOURIER-TRANSFORM ESR

*K. P. Dinse, M. Plüschau, G. Kroll, T. Prisner*  
*Institut für Physik*  
*Universität Dortmund, D4600 Dortmund 50*

and

*H. van Willigen*  
*Chemistry Department*  
*University of Massachusetts, Boston, Mass. 02125*

## 1. Introduction

Photochemical reactions in liquids generally produce anomalous populations of electron spin sublevels in free radical products. This transient deviation of populations from Boltzmann values is termed Chemically Induced Dynamic Electron Spin Polarization (CIDEP) or Electron Spin Polarization (ESP) when monitored by ESR, and has been subject of intensive research. The observed effects can be described invoking two different mechanisms. One considers the effect of optically-generated triplet precursor polarization, and takes account of the one-to-one correlation of eigenstates in the coupled representation of radical pair states and free radical spin states (Triplet Mechanism (TM)). The second one invokes the effect of spin state evolution in an transient radical pair, by which the population difference of the singlet and one of the triplet sublevels ( $S=1$ ,  $M_S=0$ ) is converted into observable ESP of the product radicals (Radical Pair Mechanism (RPM)) /1/.

In two recent publications /2,3/ we have demonstrated that the method of Fourier-transform ESR (FT-ESR) is particularly suited for the investigation of transient radicals encountered in ESP. This results from the fact that radicals can be time-labeled with high precision by a short (15 ns) microwave pulse with respect to the initiating laser pulse. Magnetic resonance of

these selectively time-marked radicals is subsequently observed via their Free Induction Decay (FID), which is determined by the unperturbed spin Hamiltonian. Additionally generated radicals can influence the FID under study only indirectly, for instance via relaxation effects like spin exchange. ESR spectra with optimum frequency resolution can be obtained for every selected delay time, because the observation time  $t$  for the FID can be chosen as  $t \gg T_2$ , independent of the delay time.

Our study was concerned with the electron transfer from photo-excited triplet zinc tetraphenylporphyrin (ZnTPP) to duroquinone (DQ) and benzoquinone (BQ). The characteristic time scale of the non-Boltzmann ESR intensities in low-viscosity solvents is in the range of 10 to 100 ns. This time scale is determined mainly by the rate of encounter of (triplet) donor molecules with acceptor molecules and by the triplet spin-lattice relaxation time of the not-directly observed precursor molecules. The life time of the  $ZnTPP^+ \cdot DQ^-$  spin-correlated radical pair, responsible for the RPM polarization pattern, can be estimated again as 10 to 100 ns, depending on solvent viscosity and on the assumption of a cut-off distance for the exchange interaction  $J(R)$ . The higher value estimate is based on a translational diffusion constant  $D_t = 10^{-6} \text{cm}^2 \text{s}^{-1}$  (as appropriate for our

experimental conditions) and a cut-off distance of  $2 \cdot 10^{-7}$  cm, corresponding to 5 times the reaction distance of the charge transfer process (see below).

Because of the order-of-magnitude improvement in time resolution of FT-ESR compared to time-resolved experiments based on transient nutation techniques, it seemed feasible to detect unambiguously the characteristic features of ESR transitions of the correlated radical pair in addition to signals resulting from the standard polarization mechanisms. The results of several conventional time-resolved ESR studies indicated that signals from radical pairs can be identified by the appearance of dispersion-like signals even under the condition of monitoring only the absorption component of the ESR signal. The appearance of field derivative-type signals in addition to the expected absorptive or emissive Lorentz lines was attributed to the superposition of absorption and emission lines with equal amplitudes, separated by the exchange interaction  $2J$  of the spin-correlated pair. Although first examples were discussed for radical pairs under condition of restricted diffusion in micelles /4,5/, later reports essentially gave the same spectral signatures also for reactions in homogeneous media /6,7/. The same model was also invoked to explain "irregular" line shapes in immobilized radical pairs, characteristic for photosynthetic reaction centers /8-10/.

Obviously, the FT-ESR technique is well adapted to settle unambiguously the question, if true dispersive signal components give rise to the derivative-type lineshapes, as was suggested already in the first publication about this problem /4/. As will be shown in this communication, the FT-ESR method with its inherent

decoupling of observation and excitation, converts transient contributions to the spin Hamiltonian of the short-lived radical pairs into a permanent phase encoding of the quasi infinitely-lived product radicals, thus allowing a convenient "read-out" of the average of the exchange interaction. The observation of transverse product radical magnetization derived from microwave-induced transitions in the spin-correlated radical pair constitutes a new independent channel for ESP, which will be present under all experimental conditions.

## 2. Experimental

FT-ESR spectra were taken with a home-built spectrometer /3/. For a better control of artefacts like zero-frequency and image peaks, a CYCLOPS /11/ phase cycling routine was installed. Long term time stability of the ESR resonance condition, which is mandatory for the phase analysis of the FID transients was ensured by using a field-frequency lock. In order to allow for an accurate phase determination of the individual hyperfine components in the product  $BQ^-$  ESR spectrum, a linear prediction (LPSVD) routine /12-14/ was used for a reconstruction of the missing part of the FID. Fig. 1 documents the base line improvement obtained, when extrapolating the first 200 ns of the FID. (The apparent dead time of the spectrometer was 100 ns, however the base line reconstruction improved when discarding additional data points, indicating remaining non-linearities of the receiver channel after overload.) Remaining phase distortions due to the finite band width of the cavity were approximately compensated by a quadratic phase correction routine. The parameter set for this correction was determined by using the fully

thermalized spectrum at large delay times and were kept constant for the analysis of all the other spectra.

Thoroughly degassed solutions of  $5 \cdot 10^{-4}$  M ZnTPP and  $5 \cdot 10^{-3}$  M BQ and DQ, respectively, in ethanol were prepared on a high-vacuum line. For an investigation of the radical-pair contributions, BQ instead of DQ was chosen because of its fewer lines, although the same "dispersive" lines had also been observed for DQ<sup>-</sup>/3/. Under conditions of laser excitation with 1 mJ pulses at 600 nm, sealed samples could be used for about 100 hours at 40 Hz repetition rate, before additional ESR lines revealed sample degradation.

### 3. Results and discussion

The accepted explanation for the generation of spin-polarized product radicals requires that the radicals are created as spin-correlated radical pairs in a well defined spin multiplicity and that, before diffusing apart, they experience a time-varying electron exchange interaction  $J$  in combination with a different Larmor frequency. In addition to this RPM scenario there is the conceptionally simpler TM, which adiabatically converts the Boltzmann polarization of the triplet precursor to both radicals. Both polarization routes have in common that the microwave field is only probing the generated polarization and one assumes that the observation via ESR is performed under conditions of negligible  $J$ . As was pointed out by various authors /4-7,9/, the time interval in the life cycle of the radicals for which  $J$  is neither dominating nor vanishing, deserves special attention. If the nuclear spin states of both radicals are assumed constant during the experiment, the radical pair

can be described by an effective spin Hamiltonian

$$H/\hbar = \omega_1 S_{1z} + \omega_2 S_{2z} - J(2S_1 \cdot S_2 + 1/2) \quad (1)$$

By  $\omega_i$  we denote the Larmor frequencies of the separated radicals including  $g$ -factor contributions as well as nuclear spin-dependent hyperfine fields. The exchange term  $J$  will be strongly dependent on radical distance and relative orientation. In the coupled representation the Hamiltonian blocks into a  $1 \times 1 \times 2$  matrix with the following eigenvalues:

$$\begin{aligned} E_1 &= -J + (\omega_1 + \omega_2)/2 \\ E_2 &= \{J^2 + (\omega_1 - \omega_2)^2/4\}^{1/2} \\ E_3 &= -E_2 \\ E_4 &= -J - (\omega_1 + \omega_2)/2 \end{aligned} \quad (2)$$

This solution is valid for all values of  $J$ , and can therefore be used to correlate the eigenfunctions in the coupled basis (appropriate for a description with dominating  $J$ ) to the product states, describing a fully separated pair with  $J=0$ . It is easily shown that the eigenstates  $|S=1, M_S=0\rangle$ ,  $|S=0, M_S=0\rangle$ , corresponding to levels 2 and 3, are correlated with product states of opposite spins  $|\alpha(1)\rangle|\beta(2)\rangle$  and  $|\beta(1)\rangle|\alpha(2)\rangle$ , respectively. If the radical pair is for instance generated in its triplet state, all three triplet sublevels will be equally populated (neglecting small deviations of the order of  $10^{-2}$ ). A subsequent fast non-adiabatic decrease of  $J$  towards zero will result in equal populations of the  $|\alpha(1)\rangle|\beta(2)\rangle$  and  $|\beta(1)\rangle|\alpha(2)\rangle$  levels. Although these levels are generated with half the population as compared to  $|\alpha(1)\rangle|\alpha(2)\rangle$  and  $|\beta(1)\rangle|\beta(2)\rangle$ , evaluation of  $S_{1z}$  and  $S_{2z}$  shows a vanishing  $z$  magnetization for both product radicals, in agreement with the standard scenario.

Under the condition of  $0 < |J| \ll |\omega_1 - \omega_2|$ , a J-split doublet is predicted for each product radical, i.e., every hyperfine component in the isolated radicals is replaced by a doublet, separated by  $2J$ . Taking into account the 2:1:1:2 level populations after non-adiabatic reduction of  $J$  into the specified range, an absorption/emission pattern is predicted in accordance with ref. /4,5/. (We listed the level populations according to their energy ordering.) Using FT-ESR the transient nature of the radical pair spectrum can be mapped into an observable, as is depicted schematically in Fig. 2. Here it is indicated that the microwave pulse rotates the anti-parallel magnetization vectors of a representative J-doublet into the transverse plane. If described in a frame rotating with the Larmor frequency of the corresponding isolated radical, both components will precess with frequencies of equal amplitude and opposite sign. Assuming that  $J$  is effective only for a short time period  $t_j$  with  $|J \cdot t_j| \ll \pi$  before cage escape renders  $J=0$ , a small magnetization component parallel to the direction of the microwave field is generated. This gives rise to a dispersive component of the FID in addition to absorptive components originating from standard RPM and TM contributions. The magnitude of the dispersive signal  $M_{\text{disp}}$  is determined by the time-integrated exchange term

$$M_{\text{disp}} = 2 \sin \left( \int_t^{t'} J(\tau) \cdot d\tau \right) \cdot M(t) \quad (3)$$

Here  $M(t)$  denotes the absolute magnetization corresponding to one of the fully separated transitions in the particular J-doublet,  $t$  marks the application of the microwave pulse, and  $t'$  describes the time after which the radicals are fully separated.

An estimate for  $(t'-t)$  can be obtained from the self-diffusion constant of the solvent. At 220 K one finds  $D = 10^{-6} \text{ cm}^2 \cdot \text{s}^{-1}$  for ethanol and using this value for the  $\text{BQ}^-$  radical also, a separation time of 100 ns is deduced, when specifying a cut-off distance of  $3 \cdot 10^{-7} \text{ cm}$  for  $J \approx T_2^{-1}$ . This value is comparable to the spectrometer dead time and explains, why within experimental error only the spectrum of the free radical is observed. A more quantitative discussion of the separation dynamics of the radical pair will be published elsewhere /15/. Utilizing the estimated value for  $(t'-t) \approx 100 \text{ ns}$ , and the experimentally determined value for  $M_{\text{disp}} \approx M_{\text{TM}} \approx 5 \cdot M_{\text{Boltzmann}}$ , as well as  $M(t) = 0.5$ , the diffusion-averaged exchange interaction is estimated as  $\int J(\tau) \cdot d\tau \approx 5 \cdot 10^{-3} \text{ rad}$ . This value agrees within one order-of-magnitude with a predicted value, when using an exponential dependence of  $J$  on the radical separation /15/.

The dispersive signal amplitude  $M_{\text{disp}}$  including its build-up and decay is determined from a set of FT-ESR spectra with different delay, which were obtained from FID's completed with LP-reconstructed segments from 0 to 200 ns. Each individual line was characterized by its amplitude and phase in the absorption /dispersion reference frame. In Fig. 3 the time dependence of the dispersive signal component is depicted as a function of delay time between laser and microwave pulse. As expected, after an initial fast rise the amplitude decreases towards zero, indicating the disappearance of spin-correlated radical pairs. In contrast to the absorption signal components, which are subject to decay via spin-lattice relaxation ( $T_{1e} \approx 10 \mu\text{s}$ ), the dispersive signal directly maps the concentration of radical pairs, which decay

via cage escape. The radical pair concentration  $c_{RP}$  is described by a two-step reaction of radical encounter and separation, which gives rise to a difference of two exponentials with equal amplitudes:

$$c_{RP} \sim \exp(-k_e t) - \exp(-k_d t) \quad (4)$$

Here first-order reaction rates with rate constants  $k_e$  and  $k_d$  for encounter and diffusive separation, respectively, are anticipated. As is seen in the figure, the data can be reasonably described by this model. A full analysis of the data and their comparison with the RPM and TM kinetic data is in progress.

#### 4. Conclusion

FT-ESR in combination with advanced data analysis enables the detection of build-up and decay kinetics of not only long-lived product radicals, but also of transient reaction intermediates like spin-correlated radical pairs in a charge-transfer reaction in solution. The contribution of the short-lived ( $\approx 100$  ns) intermediate is encoded as a phase information of the final product radical, and can be separately determined for each hyperfine component. The further information obtained from the nuclear spin dependence unambiguously determines the nature of this new ESP process. Its analysis in combination with the RPM and TM contributions will lead to a microscopic model of the photo-initiated charge transfer reaction in solution, because not only the initial encounter step but also the final cage escape can be monitored.

#### Acknowledgement

This research was supported by the DFG, and was greatly facilitated by a NATO Collaborative Research Grant. One

of us (HvW) gratefully acknowledges financial support by the Division of Chemical Sciences, Office of Basic Energy Sciences of the U.S. Department of Energy (Grant No. DE-FG02-84ER13242).

#### References

1. Time Domain Electron Spin Resonance, L. Kevan and R.N. Schwartz, Eds., Wiley, New York (1973)
2. T. Prisner, O. Dobbert, K.P. Dinse, and H. van Willigen, *J. Am. Chem. Soc.* 110, (1988) 1622
3. M. Plüschau, A. Zahl, K.P. Dinse, and H. van Willigen, *J. Chem. Phys.* 90, (1989) 3153
4. G.L. Closs, M.D.E. Forbes, and J.R. Norris, *J. Phys. Chem.* 91, (1987) 3592
5. C.D. Buckley, D.A. Hunter, P.J. Hore, and K.A. McLauchlan, *Chem. Phys. Lett.* 135, (1987) 307
6. K. Tominaga, S. Yamauchi, and N. Hirota, *J. Chem. Phys.* 88, (1987) 553
7. K. Tominaga, S. Yamauchi, and N. Hirota, *Chem. Phys. Lett.* 149, (1988) 32
8. M.C. Thurnauer and J.R. Norris, *Chem. Phys. Lett.* 76, (1980) 557
9. P.J. Hore, D.A. Hunter, C.D. McKie, and A.J. Hoff, *Chem. Phys. Lett.* 137, (1987) 495
10. D. Stehlik, C.H. Bock, and J. Petersen, *J. Phys. Chem.* - in print -
11. D.J. Hoult and R.E. Richards, *Proc. Roy. Soc. London A344*, (1975) 311
12. D. van Ormondt, private communication
13. B.J. Sullivan and Bede Liu, *IEEE TASSP* 32, (1984), 1201
14. A. Heuer and U. Haeberlen, *J. Magn. Reson.* - in print -
15. M. Plüschau, G. Kroll, K.P. Dinse, and H. van Willigen, to be published

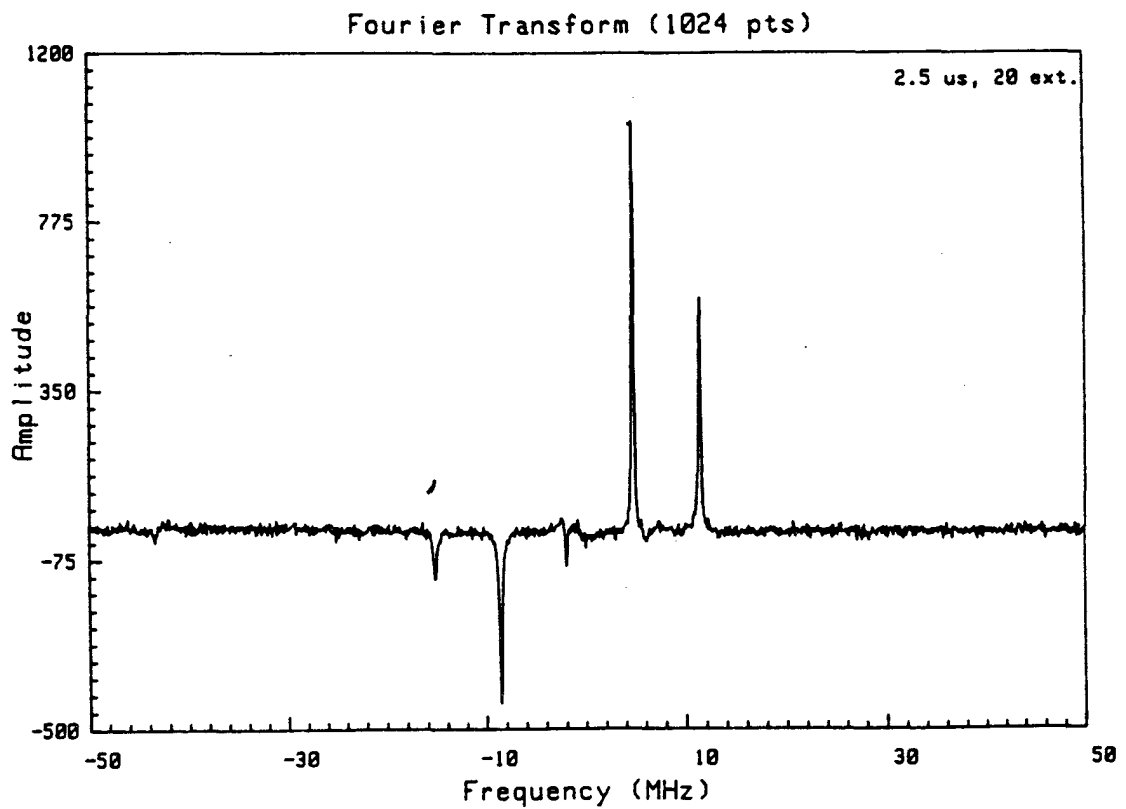
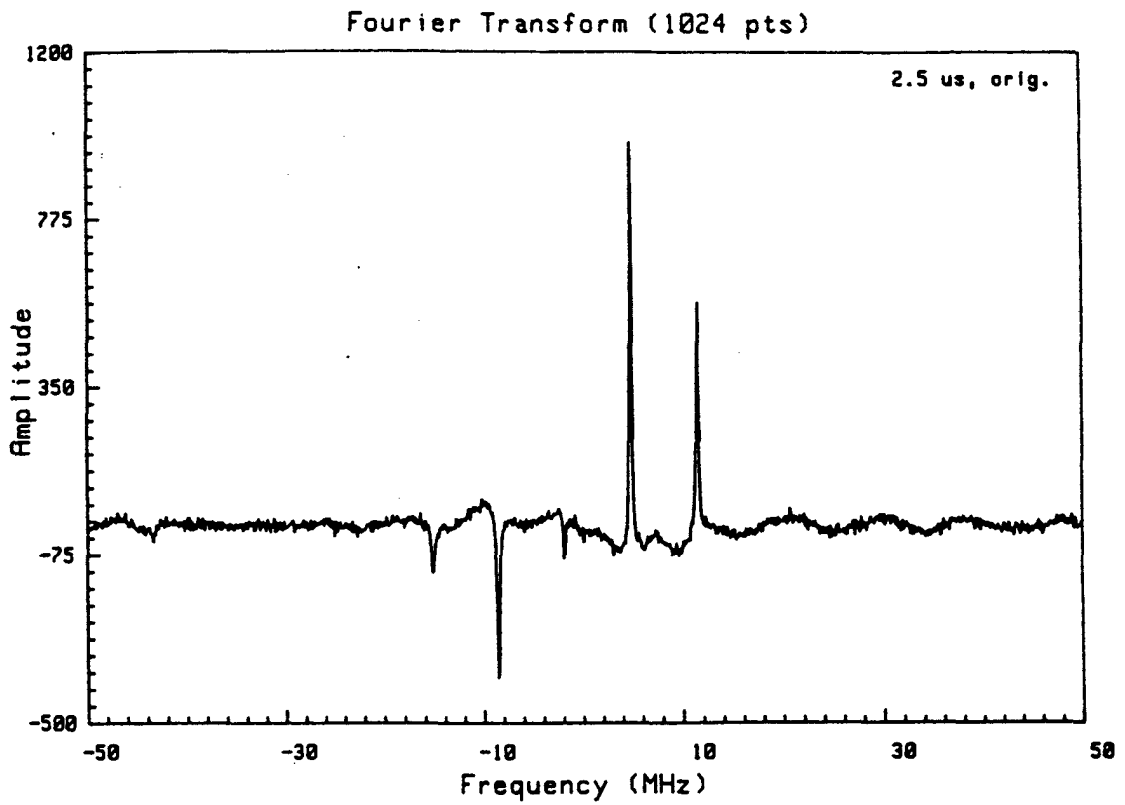
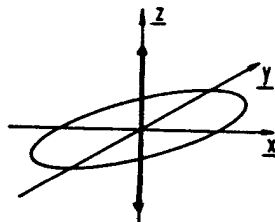
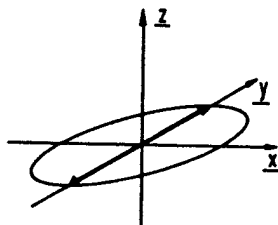


Fig. 1 Base line improvement by using a hybrid FID, consisting of the original data plus LP-reconstructed data points from 0 to 200 ns.

a) Magnetization of a J-split doublet



b) Preparation of transverse magnetization by a  $\pi/2$ -pulse parallel to x



c) Evolution of the dispersive component of the transverse magnetization

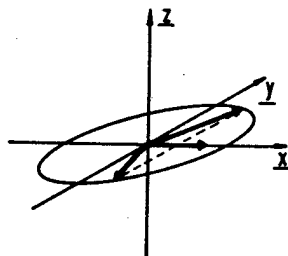


Fig. 2 Development of a dispersive signal component characteristic for an ESR transition excited in the radical pair.

### Dispersive Component

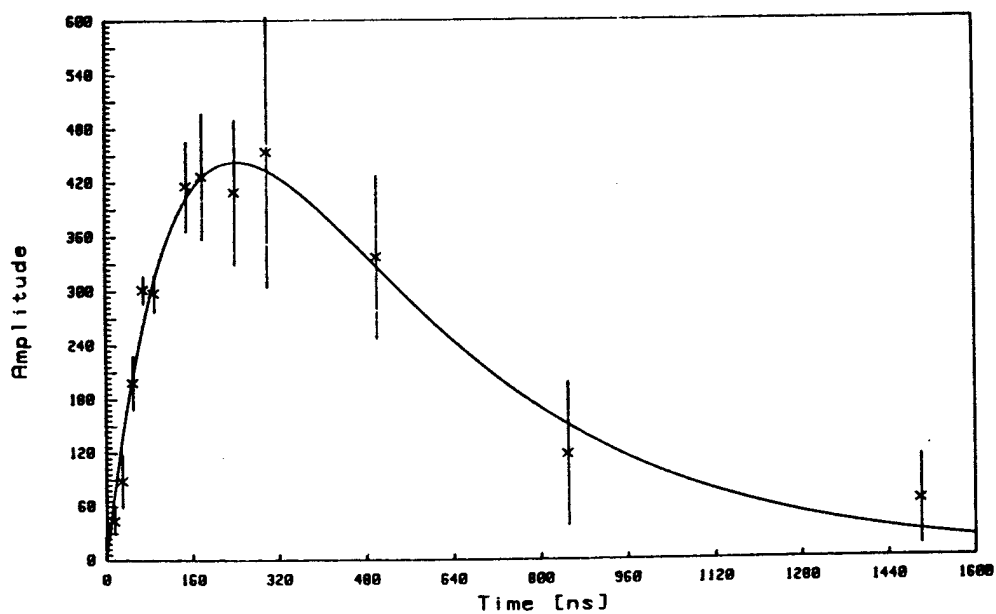


Fig. 3 Dispersive signal component for  $M = -1$  fitted to the difference of two exponential decays with equal amplitude ( $k_d = 6.1 \cdot 10^6 \text{ s}^{-1}$ ,  $k_e = 2.6 \cdot 10^6 \text{ s}^{-1}$ ).